

Holographic Recording in Cross-Linked Polymeric Matrices through Photoacid Generation

Anzar Khan,[†] Luis M. Campos,[†] Alexander Mikhailovsky,[‡] Muhammet Toprak,[‡]
Nicholas C. Strandwitz,[§] Galen D. Stucky,^{*,†,‡,§} and Craig J. Hawker^{*,†,‡,§}

Department of Chemistry and Biochemistry, Materials Department, Materials Research Laboratory, and
Mitsubishi Chemical Center for Advanced Materials, University of California,
Santa Barbara, California 93106-9510

Received February 20, 2008. Revised Manuscript Received March 24, 2008

We report a novel strategy for writing volume holograms by photoacid generation and subsequent acid-catalyzed degradation leading to increased free volume/refractive index modulation in the exposed regions of a cross-linked rigid polymeric matrix. This strategy offers nondestructive read out and high diffraction efficiency and allows optical-quality, millimeter thick films to be fabricated that possess excellent thermal and dimensional stability. A key feature of this approach is the efficient acid-catalyzed degradation of functional groups in the cross-linked matrix leading to release of volatile products which diffuse readily out of the thick films. Furthermore, the reported data storage material is lightweight and inexpensive and can be easily processed into different shapes, making it an attractive candidate for data storage applications.

Introduction

The ever-increasing demand for high-capacity data storage systems has stimulated tremendous research during the past few years into alternative technologies such as probe-based systems,¹ phase change devices,² etc. One of the most promising approaches is holographic data storage,^{3–7} which meets future information storage needs and significantly benefits from the information being stored throughout the volume of a storage medium. This strategy of recording data in three dimensions provides a unique opportunity to encode ultrahigh storage density in a small volume form factor. The emerging field of volume holography is however faced with the challenge of developing suitable materials that meet all the stringent requirements for commercial viability. These requirements include high photosensitivity, nondestructive readout, dimensional stability, high optical quality, good dynamic range, and low cost.

Over the last five decades, a variety of optical systems have been developed for holographic devices with the constant limiting factor being materials performance. The materials that have been surveyed include inorganic photo-refractive crystals, which offer nondestructive read out capabilities^{8,9} and high optical quality but suffer from low

sensitivity and are limited by the dependence on growing single crystals. Similarly, photoresponsive oligomers,¹⁰ polymers,^{11–15} and dendrimers¹⁶ have been investigated. Although these materials display high birefringence and ease of processing, they are limited by destructive read out and low sensitivity. Photopolymers,^{17–20} on the other hand, exhibit excellent sensitivity and high dynamic range, but a number of issues hamper their practicality of use. Such issues include writing-induced shrinkage of the material and short shelf life of the holographic media. In this manuscript, we report a novel use of photoacid generation and subsequent chemical modification of preformed cross-linked thick films for high-performance holographic storage. Significantly, this approach does not rely on either monomer diffusion or

- (9) Hesselink, L.; Orlov, S. S.; Liu, A.; Akella, A.; Lande, D.; Neurgaonkar, R. R. *Science* **1998**, *282*, 1089–1094.
- (10) Berg, R. H.; Hilvested, S.; Ramanujam, P. S. *Nature* **1996**, *383*, 505–508.
- (11) Meerholz, K.; Volodin, B. L.; Sandalphon; Kippelen, B.; Peyghambarian, N. *Nature* **1994**, *371*, 497–500.
- (12) Kippelen, B.; Marder, S. R.; Hendrickx, E.; Maldonado, J. L.; Guillemet, G.; Volodin, B. L.; Steele, D. D.; Enami, Y.; Sandalphon; Yao, Y. J.; Wang, J. F.; Rokel, H.; Erskine, L.; Peyghambarian, N. *Science* **1998**, *279*, 54–57.
- (13) Liphard, M.; Goonesekera, A.; Jones, B. E.; Ducharme, S.; Takacs, J. M.; Zhang, L. *Science* **1994**, *263*, 367–369.
- (14) Yoneyama, S.; Tsutsumi, O.; Kanazawa, A.; Shiono, T.; Ikeda, T. *Macromolecules* **2002**, *35*, 8751–8758.
- (15) Hackle, M.; Kador, L.; Kropp, D.; Schmidt, H. W. *Adv. Mater.* **2006**, *19*, 227–231.
- (16) Lohse, B.; Vestberg, R.; Ivanov, T. M.; Hvilsted, H.; Berg, R. H.; Ramanujam, P. S.; Hawker, C. J. *J. Polym. Sci., Part A: Polym. Chem.* **2007**, *45*, 4401–4412.
- (17) Close, D. H.; Jacobson, A. D.; Margerum, J. D.; Brault, R. G.; Mcclung, F. J. *Appl. Phys. Lett.* **1969**, *14*, 159–160.
- (18) Trentler, T. J.; Boyd, J. E.; Colvin, V. L. *Chem. Mater.* **2000**, *12*, 1431–1438.
- (19) Schilling, M. L.; Colvin, V. L.; Dhar, L.; Harris, A. L.; Schilling, F. C.; Katz, H. E.; Wysocki, T.; Hale, A.; Blyler, L. L.; Boyd, C. *Chem. Mater.* **1999**, *11*, 247–254.
- (20) Dhar, L.; Hale, A.; Katz, H. E.; Schilling, M. L.; Schnoes, M. G.; Schilling, F. C. *Opt. Lett.* **1999**, *24*, 487–489.

* To whom correspondence should be addressed. E-mail: hawker@mrl.ucsb.edu, stucky@chem.ucsb.edu.

[†] Materials Research Laboratory.

[‡] Department of Chemistry and Biochemistry.

[§] Materials Department.

- (1) Gotsmann, B.; Duerig, U.; Frommer, J.; Hawker, C. J. *Adv. Funct. Mater.* **2006**, *16*, 1499–1505.
- (2) Wuttig, M.; Yamada, N. *Nat. Mater.* **2007**, *6*, 824–832.
- (3) Gabor, D. *Nature* **1948**, *161*, 777–778.
- (4) Gabor, D. *Science* **1972**, *177*, 299–313.
- (5) Psaltis, D.; Mok, F. *Sci. Am.* **1995**, 70–76.
- (6) Coufal, H.; Psaltis, D.; Sincerbbox G.; Eds. *Holographic Data Storage*; Springer-Verlag: New York, 2000.
- (7) Psaltis, D. *Science* **2002**, *298*, 1359–1363.
- (8) Buse, K.; Adibi, A.; Psaltis, D. *Nature* **1998**, *393*, 665–668.

reversible photochemical reactions to achieve refractive index modulation, which overcomes many of the traditional issues associated with photopolymers.

Experimental Section

Materials. All chemicals were purchased from Aldrich and used as received.

Sample Preparation. Solutions were prepared by mixing 325 mg of *tert*-butyl 4-vinylphenyl carbonate, 3.5 mg of 2,2'-azobis(2-methylpropionitrile) (AIBN), 38 mg of divinylbenzene, 20 mg of isopropyl-9*H*-thioxanthen-9-one, and 20 mg of [4-[(2-hydroxytetradecyl)oxy]phenyl]phenyliodonium hexafluoroantimonate. The mixture was placed in an oil bath (90 °C) for a few seconds until a clear yellow solution was obtained. This solution was then passed through a 0.45 μm pore size filter. Note: Special care should be taken to avoid moisture uptake by the sample.

To fabricate optical films, several drops of the filtered yellow solution were placed between two clipped 3 \times 1 in. microscope slides separated by Teflon spacers of the desired thicknesses (0.5–1.5 mm). The assembly was then placed in an oven at 110 °C. A curing time of 40 min was required to obtain good optical-quality films of 0.5 mm thickness. After curing the films, one glass slide was carefully removed. The sample was mounted on the holographic setup and exposed through the open face of the sample.

Hologram Recording and Evaluation. The experimental setup for recording of holograms was assembled on an optical table suspended on vibration-damping supports (Newport I-2000) and further enclosed to minimize airflow and dust during the recording process. The output of a blue diode laser (Crystalaser BCL-040-405-S, 407 nm, 40 mW, single longitudinal mode) was split into two beam with equal power using a continuously adjustable beam splitter consisting of two half-wavelength plates and a polarizer cube.²¹ The resulting beams passed through spatial filters and collimating lenses producing beams with a diameter of \sim 10 mm. The angle between the recording beams was 36.6°. The optical power density in a single recording beam was \sim 3 mW/cm². A sample was placed at the intersection point of the recording beams on a computer-controlled rotation stage (Newport URS75PP, 0.016° positioning accuracy). The axis of the sample rotation was perpendicular to the plane determined by the recording beams. A probe beam was generated by a low-power (<1 mW) He–Ne laser emitting at 632.8 nm. The probe beam was aligned on the sample at the Bragg's angle. The power of the probe beam was adjusted by a neutral density filter wheel to avoid saturation of the detectors. In order to monitor the intensity of diffracted and transmitted probe beams, the output of the He–Ne laser was modulated by an optical chopper (SRS SR540). The intensity of the beams passing through the sample was measured by large-area Si photodiodes protected from ambient light and the recording beams by interference filters. Signals from the photodiodes were amplified by a transimpedance amplifier (SRS SR570) and fed into a digital lock-in amplifier (SRS SR830) synchronized with the chopper. Exposure of a sample to the recording beams was controlled by a computer-operated shutter (Uniblitz CS25). The experimental setup allowed for control of the amount of optical energy used for the recording of a hologram and the recording of multiple diffraction gratings on the same spot (M# measurements) while also allowing the measurement of angular selectivity for diffraction gratings (determination of diffraction efficiency).

Recording of single holograms was performed at the sample orientation when the angles of incidence for the two recording

beams were equal and the recorded grating vector was parallel to the sample surface. The recording laser shutter was opened for a user-defined amount of time, and monitoring of the diffracted beam intensity started simultaneously. The diffraction efficiency, η , was determined using the following formula

$$\eta = \frac{I_D}{I_D + I_T} \quad (1)$$

Here, I_D and I_T are intensities of diffracted and transmitted beams, respectively. It was assumed that the material was transparent at the wavelength of the probe laser. Holograms recorded in the experiments are transmission volume holograms (transmission Bragg holograms),¹⁹ and their diffraction efficiency for a beam with the angle of incidence equal to the internal Bragg's angle, θ , can be obtained by

$$\eta = \sin^2 \frac{\pi n_1 d}{\lambda \cos \theta} \quad (2)$$

where n_1 is the photoinduced modulation of the refractive index, d is the thickness of a hologram, and λ is the wavelength of the probe light. From eq 2 one can determine the photoinduced modulation of the refractive index. The sensitivity, S , of the material was estimated using the following equation

$$S = \frac{\sqrt{\eta}}{dtI} \quad (3)$$

Here, t is the recording time and I is the combined intensity of recording beams. Multiplexing capabilities of the recording material were evaluated using the M# parameter

$$M\# = \sum_{i=1}^N \sqrt{\eta_i} \quad (4)$$

In M# measurements, N holographic gratings were recorded consecutively on the same spot in the sample. The sample was rotated by a certain angle between the recordings. For each hologram, the diffraction efficiency, η_i , was obtained. The holographic grating period, Λ , was calculated using the following formula

$$\Lambda = \frac{\lambda}{2 \sin(\phi/2)} \quad (5)$$

Here, λ is the recording laser wavelength and ϕ is the angle between the recording laser beams. In our case, $\lambda = 407$ nm and $\phi = 33.6^\circ$; hence, a theoretical holographic grating period of $\Lambda = 704$ nm was calculated.

Results and Discussion

In holographic data storage, information is stored in the form of an optical interference pattern. This interference pattern is created by the intersection of two coherent optical beams which causes alteration in the physical or chemical properties of the recording medium. Typically, this alteration is a change in the refractive index of the material and refractive index contrast between the bright and the dark regions of the holographic media determines the strength of a volume hologram. It was anticipated that increasing the free volume in the bright regions of the holographic media via the catalytic decomposition of functional groups attached to the backbone of a cross-linked polymer matrix would lead to the evolution of volatile small molecules and a significant

(21) Hariharan, P. *Optical Holography Principles, Techniques, and Applications*, 2nd ed.; Cambridge University Press: New York, 1996.

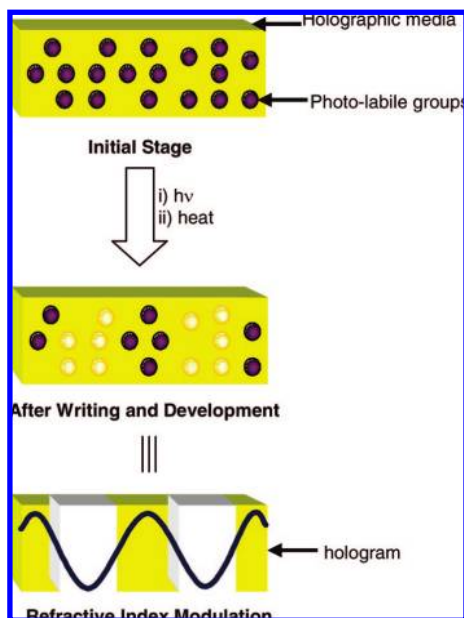


Figure 1. Schematic illustration of the chemically amplified three-dimensional imaging system. Fabrication of a thick film containing acid-labile free-volume generators (FVG) and the data writing process via (i) laser-induced acid generation and protonation of the FVG groups in the bright regions; (ii) development of the hologram by a postexposure baking treatment, resulting in refractive index modulation.

change in the refractive index of the material (Figure 1).^{22–25} This release of gaseous products capable of diffusing out of the matrix is anticipated to result in either increased free volume or generation of nanopores filled with air. Incorporation of air (dielectric constant 1.01) in a higher dielectric constant rigid polymeric matrix should result in significant modulation of the refractive index. To explore this design strategy, the widely studied chemically amplified,^{26–29} acid-catalyzed decomposition of carbonate functionalities was exploited to generate increased free volume and a concurrent reduction in refractive index. The optimized holographic system is therefore composed of four components: (a) a cross-linkable molecule containing the acid-labile *tert*-butoxycarbonyl (*t*-BOC) group as free-volume generator (FVG), (b) a cross-linker that leads to thick film formation as well as dimensional stability, (c) a photoacid generator (PAG),³⁰ and (d) a sensitizer for enhanced reactivity at the writing at wavelength of 407 nm.

This strategy relies on a series of well-studied chemical reactions that form the basis of modern photolithography.³¹

(22) Maex, K.; Baklanov, M. R.; Shariyran, D.; Lacopi, F.; Brongersma, S. H.; Yanovitskaya, Z. H. *J. Appl. Phys.* **2003**, *93*, 8793–8841.

(23) Hedrick, J. L.; Miller, R. D.; Hawker, C. J.; Carter, K. R.; Volksen, W.; Yoon, D. Y.; Trollsas, M. *Adv. Mater.* **1998**, *10*, 1049–1053.

(24) Abdallah, J.; Silver, M.; Allen, S. A. B.; Kohl, P. A. *J. Mater. Chem.* **2007**, *17*, 873–885.

(25) One possible contributor to the final refractive index modulation would be the inherent refractive index difference between the *t*-BOC- and hydroxy-containing cross-linked polymer.

(26) Macdonald, A. S.; Willson, C. G.; Fréchet, J. M. J. *Acc. Chem. Res.* **1994**, *27*, 151–158.

(27) Willson, C. G.; Ito, H.; Fréchet, J. M. J.; Houlihan, F. *Proc. IUPAC, IUPAC Macromol. Symp.* **1982**, *28*, 448.

(28) Ito, H.; Willson, C. G. *Polym. Eng. Sci.* **1983**, *23* (18), 1012.

(29) Ito, H.; Willson, C. G.; Fréchet, J. M. J. U.S. Patent 4491628, 1985.

(30) Crivello, J. V. *J. Polym. Sci., Part A: Polym. Chem.* **1999**, *37*, 4241–4254.

(31) Ito, H. *IBM J. Res. Develop.* **2000**, *44*, 119–130.

The first event in this recording system is the light-induced decomposition of the PAG which produces a strong acid in bright regions of the holographic media. As a result, a replica of the interference pattern is stored as a latent image in the recording material. Upon baking, the dissolved acid in the exposed regions catalyzes the decomposition of the *t*-BOC groups with the release of carbon dioxide and isobutene (both gaseous products). Diffusion of these gases out of the film leads to formation of free volume/porosity and a decrease in the refractive index in exposed regions. This refractive index modulation, as a result of the photochemical decomposition, results in inscription of the hologram. Significantly, the catalytic nature of the decomposition reaction makes the system highly sensitive with one photon triggering a chain reaction, resulting in the decomposition of many carbonate groups. This high sensitivity translates to rapid response of the system to the writing process, and hence, only short recording times are required for storing each hologram.

Iodonium salt **1** and isopropyl-9*H*-thioxanthen-9-one **2** were chosen as PAG and sensitizer, respectively (Figure 2), due to their high solubility in the nonpolar matrix material and low absorption cross-section of the sensitizer at 407 nm. This high solubility allows for fabrication of thick films by solventless processing without phase separation during the curing process. High optical-quality films with variable thicknesses of up to 1.5 mm were therefore fabricated under thermal conditions by the radical-initiated (AIBN) cross-linking of FVG **3** and divinylbenzene with the PAG and sensitizer being dissolved in this cross-linked matrix.

To evaluate the performance of these materials, a single hologram was recorded by illuminating the sample with the interference pattern of two collimated 407 nm laser beams with a total optical power density of ~ 6 mW/cm² and beam diameter of ~ 10 mm. No diffraction of the probe beam could be observed after the recording.³² This is expected as the writing beams generate only trace amounts of acid in the exposed regions of the holographic media and do not result in any change of the refractive index of the material. However, development of the hologram by baking the sample revealed high diffraction efficiencies ($\sim 45\%$) (Figure 3). As in the case of photolithography, post-exposure baking provides the thermal energy necessary for acid-catalyzed cleavage of the carbonate bonds with the acid being regenerated after elimination of carbon dioxide and isobutylene and catalyzes the decomposition of other carbonate functionalities. The postexposure baking process also facilitates release of the gaseous byproduct. This series of reactions was found to lead to efficient refractive index modulation in the exposed regions with postexposure baking times being optimized by monitoring the diffraction efficiency after development.³² These studies revealed that a minimum of 5 min at 110 °C is required to obtain the maximum diffraction efficiency, while postexposure baking times longer than 30 min exhibited only a marginal further increase. After development, the presence of a hologram could be detected visually with the films diffracting ambient light. A range of colors can be seen macroscopically, indicating that a volume grating of high diffraction efficiency has been stored in the

(32) Please see the Supporting Information.

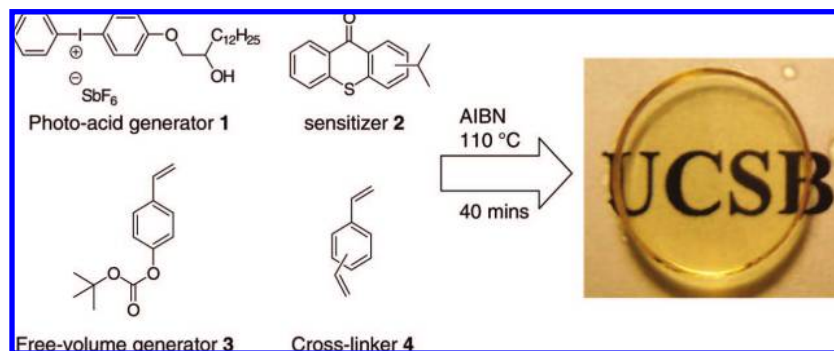


Figure 2. Chemical structures of the precursors used in the fabrication of the holographic media (left), and AIBN-assisted preparation of 1 mm thick film from these precursors by solventless processing (right).

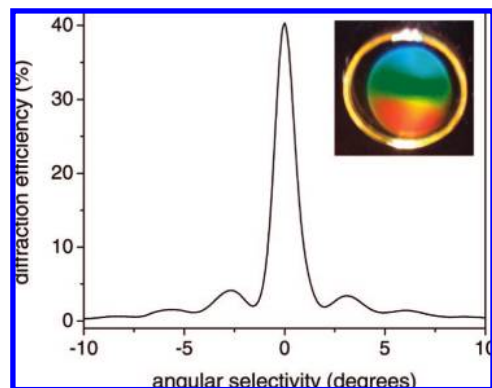


Figure 3. Angular selectivity response of a plane-wave hologram in a 0.5 mm thick film at the readout wavelength of 632.8 nm. The first-order diffraction efficiency of 43.3% corresponds to a refractive index modulation (Δn) of 2.82×10^{-4} . The inset shows the film after writing and developing the hologram. A number of colors can be seen due to the ambient light diffraction by the recorded grating. Note that the diameter of the film is larger than the diameter of the writing beams. Exposure time for recording the hologram was 180 s.

material (Figure 3, inset). A typical hologram in this material exhibits first-order diffraction efficiency in the range of 25–45% and possesses an angular bandwidth of 1.2° (full-width measured at half-maximum) at 632.8 nm (Figure 3). The angular selectivity curve exhibits well-defined nulls, indicating that the hologram is recorded throughout the bulk of the material. Two different types of control experiments³² were performed in order to confirm the central role of photogenerated acid in this process. For example, films were prepared without PAG and exposed to the holographic interference pattern. No diffraction could be observed from these samples even after post-exposure baking/development of 30 min. In another control experiment, the labile *tert*-butoxycarbonyl monomer was replaced with the unreactive *tert*-butyl styrene derivative and exposed to the interference pattern. Since *tert*-butyl styrene does not undergo acid-catalyzed decomposition, no diffraction could be detected, which demonstrates that acid-catalyzed decomposition of the carbonate groups is critical to hologram formation.

The solventless processing conditions developed permits fabrication of thick cross-linked films (thickness = 0.5 mm). This thickness of the recording media allows angular multiplexing of several holograms within the same sample. Figure 4 shows three and five angularly multiplexed holograms of approximately equal strength recorded in a 0.5 mm thick sample. Due to the relatively broad angular bandwidth

of the hologram, a minimum increment of 2° in the rotation angle was necessary to avoid cross-talk between holograms (Figure 4). The performance value that characterizes the capacity of these materials, the dynamic range ($M/\#$), was determined for these samples and found to range from 0.5 to 0.7.

To investigate the dimensional stability of the recording material, SEM cross-sectional analysis was performed on a 0.5 mm thick holographic film.³² The thickness of the film remain unchanged after recording and development of the hologram at 110 °C for 10 min. These results demonstrate that an increase in free volume does not result in physical collapse of the bulk structure as observed in the case of photoresist materials and porous dielectric materials where the pore size is 5 nm or greater. In addition, no pores could be detected in the structure, which suggests that any increase in free volume or development of porosity occurs below the detection limit of 1–2 nm. This high dimensional stability when compared to linear polymers (photoresists) can be attributed to the cross-linked nature of the matrix material.

Atomic force microscopy (AFM) measurements were performed to investigate the topography of the polymer film before and after hologram inscription. These measurements revealed that a surface relief grating (SRG) with a modulation depth of ca. 6 nm is formed in addition to the index grating (Figure 5). Formation of a SRG is most likely a result of the acid-catalyzed thermal decomposition of the less highly cross-linked polymer surface layer. The ratio of the relief height to the film thickness is very small ($\sim 0.001\%$ of total film thickness), and hence, the contribution of SRG to the refractive index grating is negligible. The AFM surface profile of the SRG allowed for the experimental correlation of the grating periodicity to the theoretical value with these measurements, revealing a grating period of ca. 700 nm (Figure 5). This observed fringe periodicity is in good agreement with the theoretically calculated grating period of 704 nm.

The holographic grating was also observed by scanning electron microscopy (SEM).³² Before recording the grating, no structural features were present on the surface of the film. However, a fringe structure composed of bright and dark regions was observed after recording the hologram. This indicates that the photoinduced decomposition of carbonate groups successfully resulted in the periodic change in material density. More importantly, the cross-sectional

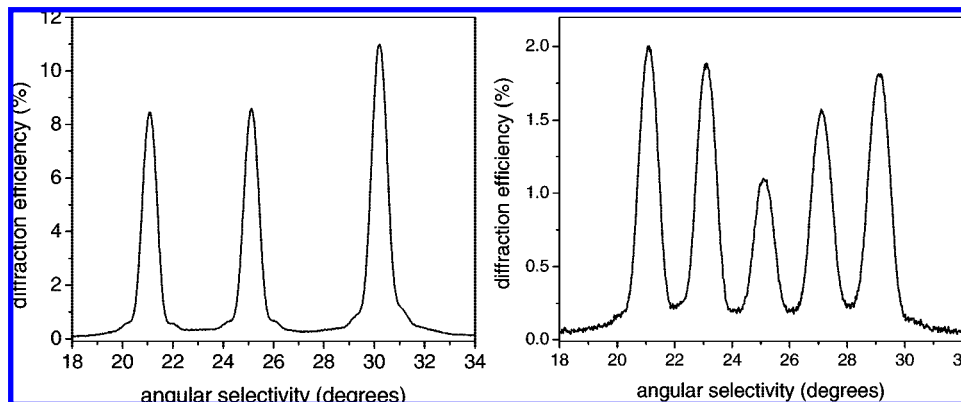


Figure 4. Angular multiplexing of 3 (left) and 5 (right) holographic gratings in a 0.5 mm thick film. The exposure time for recording each hologram was 60 and 30 s, respectively. The gratings were recorded at different angles, while the angle between the recording beams was kept constant.

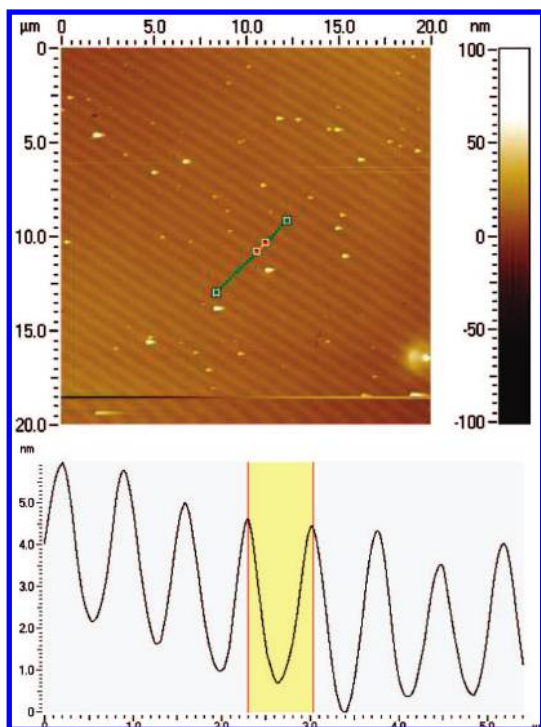


Figure 5. AFM image of the film surface after grating formation in 0.5 mm thick film (left). AFM surface profile showing the experimental grating periodicity of 700 nm (right). The angle between the two writing laser beams was set at 33.6° . This angle corresponds to a theoretical grating period (Λ) of 704 nm.

analysis of the material revealed that the periodic fringes are present throughout the depth of the material, demonstrating the volumetric nature of the recorded grating (Figure 6).

One of the most significant challenges in developing suitable, three-dimensional storage materials is to avoid the problem of destructive read out, image fade, and long-term hologram stability. Often, reading the data at the wavelength of the recording laser erases the hologram by eliminating dark regions via the same photochemical mechanism used for the hologram formation. In the present imaging system, the data is encoded in two steps: (1) photogeneration of acid and inscription of latent image and (2) development by baking to reveal and permanently store this image. The advantage of this two-step system is that the first step alone cannot write or erase data permanently and thus provides the opportunity to permanently encode or fix the holograms.

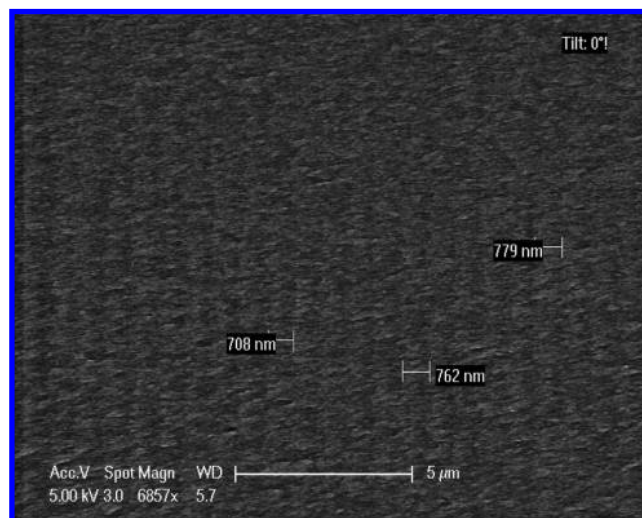


Figure 6. Cross-sectional SEM analysis of the 0.5 mm thick holographic media. The dark and bright regions can be seen throughout the depth of the material, indicating the material density change due to acid-catalyzed decomposition of the carbonate groups in the exposed regions of the holographic media. The experimental periodicity is in agreement with the calculated periodicity.

In the present system, once a hologram is thermally developed, it can be read using the writing laser source. Furthermore, the hologram is stable at room temperature given that the second step (acid catalyzed *t*-BOC decomposition reaction) requires relatively high temperatures to initiate. However, at higher temperatures the holograms are liable to erasure due to the triggering of the decomposition reaction in the presence of trace amounts of acid generated during the reading process. Hence, it is essential to consume all the PAG in the holographic media to impart thermal stability to the holograms. Thus, a strategy was devised in order to achieve nondestructive readout from the materials under investigation. After writing one or more holograms in a sample, the polymer film is homogeneously illuminated at the writing wavelength. This blanket exposure results in the complete decomposition of the remaining PAG molecules and generation of acid. The sample was then treated with ammonia vapors, which results in neutralization of all photogenerated acid present throughout the volume of the film. This treatment renders the films photochemically inert and the prerecorded holograms stable at high temperatures since no decomposition reaction can occur in the absence

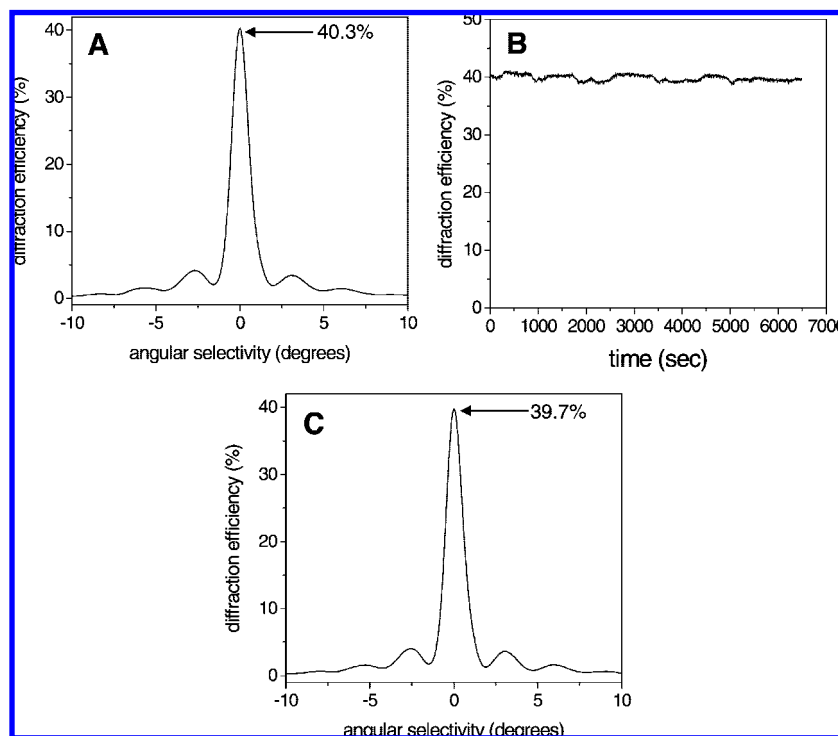


Figure 7. (A) Angular selectivity curve of a volume hologram after recording and development. (B) Real-time diffraction efficiency of the same hologram as a function of exposure time to a homogeneous 407 nm laser source. (C) Angular selectivity curve after blanket exposure, base treatment, and baking at 110 °C for 10 min.

of an acid. Figure 7B shows the diffraction efficiency measured in real time as a function of exposure time when a recorded hologram is exposed to uniform illumination at the writing wavelength (407 nm). The diffraction efficiency remains unchanged over the entire exposure period, indicating that the holograms are stable to the writing beams at room temperature. The film was then exposed to ammonia vapors for 40 min followed by baking at 110 °C for 15 min. Very little decrease ($\sim 0.5\%$) in diffraction efficiency was observed after the baking process, showing evidence that the recorded hologram is not affected by exposure to the recording beams (Figure 7). In comparison, a large decrease ($\sim 60\%$) in diffraction efficiency was observed if the base treatment is excluded after the blanket exposure.³²

Finally, in order to demonstrate the practical use of these materials, aging tests were performed at elevated temperatures to characterize the thermal stability of the hologram. After heating the sample for 60 days at 65 °C, the angular selectivity curve of the hologram remained intact and a small increase in diffraction efficiency was observed. The high thermal stability of these materials coupled with the ability to ‘fix’ the holographic image suggests that this photoacid generator approach is a viable candidate for archival data storage.

Conclusions

We successfully demonstrated that photoacid generation coupled with functional group interchange can be success-

fully utilized to achieve refractive index modulation capable of holographic information storage in thick polymeric matrices. The rapid diffusion of volatile side products from these films allows the free volume/porosity of these films to be increased, leading to a refractive index decrease in the irradiated areas. In addition, the cross-linked nature of the starting polymer films leads to significant dimensional and mechanical stability while also permitting optical-quality films that do not suffer from shrinkage issues to be easily fabricated. The stepwise nature of this process also allows ‘fixing’ of the hologram by neutralization of the acid from the exposed PAG by exposure to base before development of the latent images, leading to a high-performance, thermally stable system.

Acknowledgment. Financial support from Mitsubishi Chemical Center for Advanced Materials (MC-CAM), Mitsubishi Chemical Group Science and Technology Research Center, Inc., and the central facilities of the UCSB Materials Research Laboratory (NSF Grant DMR05-20415) is gratefully acknowledged.

Supporting Information Available: Details of SEM characterization, control experiments, absorption spectra, hologram erasure data, etc. (PDF). This material is available free of charge via the Internet at <http://acs.pubs.org>.

CM800500Q